JOURNAL OF MATERIALS SCIENCE 28 (1993) 5397–5413

Review
Synthesis of cast metal matrix particulate composites

S. RAY*
Department of Materials, University of Wisconsin-Milwaukee, Milwaukee, WI 53211, USA

The present review begins by briefly tracing history in the early days of development of cast metal-matrix composites and also outlines different casting routes for their synthesis. The problems faced by the quality of cast products and their relation to the process variables and characteristics of a given process, constitute the main theme of the review. The development of microstructure has been discussed in view of nucleation behaviour anticipated on the basis of estimated interface energies. The solidification around dispersoids and in regions away from it has been highlighted. Porosity in cast composites (its origin and control in cast components by suitable mould design) has engaged attention because of damage to mechanical properties due to porosity. The chemical reactions at the interface between dispersoid and matrix during processing of certain important systems of composites, have been described and the means of controlling these reactions have been indicated. The review concludes by drawing attention to the potential for application of cast composites in different industrial components and underlines the necessity of research in certain related fields so that industrial application of cast metal-matrix composites will soon become a reality.

1. Introduction

In the past, ceramic particles in metals and alloys were considered undesirable inclusions impairing strength and ductility. In the mid-sixties, nickel-coated graphite powders were incorporated in aluminium alloys by injecting the powders together with argon gas into a molten bath of the alloy; this marked the beginning of cast metal-matrix particulate composites (MMPC) [1]. In 1968, at the Indian Institute of Technology, Kanpur, the present author developed cast aluminium–alumina composites by incorporating alumina particles by stirring the molten alloy with an impeller as the particles were added, and thus, the process of stir-casting emerged [2]. In addition, mixing of non-wetting particles into liquid alloy was promoted by the addition of alloying elements such as magnesium, in place of the nickel coating used earlier. In the early seventies, Massachusetts Institute of Technology began the practice of introducing particles to semi-solid alloys at a temperature between those of the solidus and the liquidus [3] for the alloy. The enhanced viscosity of the semi-solid alloy increased the stability of the slurry by delaying particle flotation or settlement. At the University of Roorkee, an arrangement for bottom pouring was introduced so that slurry could be stirred until casting, there being no need to withdraw the stirrer [4].

The processes where particles are dispersed in a liquid or a semi-solid alloy, can be broadly categorized as dispersion processes [5] where the amount of particles which can be incorporated, is limited. Conventional casting of a slurry containing molten alloy and dispersoids, requires a sufficient casting fluidity. A major advantage of these processes is that MMPC components can be manufactured using the infrastructure of conventional foundries.

The efforts to overcome the limitation of particle content in cast MMPC have resulted in another set of processes where a preform or a bed of dispersoids is impregnated by molten alloy due to application of a pressure differential at the ends of a preform or a bed [5]. Three processes can be mentioned in this broad category of impregnation technique-squeeze casting, pressure infiltration, and the Lanxide process, listed in order of decreasing pressure differential generally applied in practice. The process of squeeze casting was devised in the early sixties for forming metals and alloys and combining the advantages of both casting and forging in the resultant product. The application of the squeeze-casting process to the synthesis of cast metal-matrix composites has been pioneered by Japanese research workers. The process of pressure infiltration was employed at Massachusetts Institute of Technology. The investigators at the Lanxide corporation noticed that if a molten alloy has proper alloying additions to ensure its capability to wet dispersoids, it can flow into a bed of those dispersoids under gravity [6]. This low-cost technique of

* *Present address:* Department of Metallurgical Engineering, University of Roorkee, Roorkee, Uttar Pradesh 247 667, India.

0022–2461

pressureless infiltration is called the Primex process. In 1983, Martin Marietta Corporation developed the XD process where elemental components of various reinforcing phases are mixed with the matrix alloy and a self-propagating high-temperature reaction is initiated [7].

In the late eighties, a spray-casting process, called the Osprey process, was also employed for the synthesis of cast composites. Here, molten alloy is gas atomized and co-sprayed with dispersoids on a substrate to form cast MMPC billet [8].

All the processes mentioned above, appear to have potential to evolve into manufacturing processes for industrial application of cast MMPC. But only stir-casting has so far been scaled up for regular production of metal-matrix composite ingots by Duralcan, USA, and Comalco, Australia. In spite of high priority given to the development of metal-matrix composites by different governments in their national programmes such as the Strategic Defence Initiative (SDI, USA), Basic Technologies for Future Industries (Japan), or that of the Department of Trade and Industry (DTI, UK), industrial application of metal-matrix composites has yet to begin on a regular basis. Two important reasons for this delay, as identified by Feest [9], are: (a) dampening of early excitement in the sixties by over optimistic promises and disappointing properties observed in unoptimized samples, and (b) lack of enthusiasm of traditional alloy suppliers because of a perception that development of a composite may threaten their own established markets. The main thrust of efforts to develop composites has come from three types of industries: manufacturers of reinforcing materials, industries involved in producing components, and small companies interested in exploiting specific inventions. The publicity given to the light-weight aluminium connecting rods (conrods) reinforced with alumina fibres as developed by Toyota Du-Pont collaboration [10], and the aluminium–alumina diesel piston with an enhanced resistance to thermal fatigue [11], generated widespread interest in a spectrum of industrial sectors, including automotive, defence and aerospace industries.

2. Routes of synthesis

Different processes for fabrication of cast metal-matrix particulate composites are classified in Fig. 1. In this section these methods will be briefly outlined.

2.1. Dispersion processes

Fig. 2 shows schematically the apparatus generally used for either stir-casting or compocasting. In stir-casting, the alloy is in a fully molten state when the wetting agent and the particles are stirred into it. The wetting agent will not be necessary when the particles are naturally wetted by the alloy or have a wettable coating. The process of particle transfer to the molten alloy has been analysed and the wetting angle plays a critical role [12]. In compocasting, the alloy is in semi-solid state when the particles are stirred into it and in all other respects both the processes (stir-casting and compocasting), are identical.

For a given experimental apparatus, the process variables are [13]: (i) position of stirrer, (ii) size of stirrer, and (iii) speed of stirrer. If the temperature of the melt is taken as a continuous variable across the liquidus, both the techniques can be discussed together. It is possible to stir liquid or semi-solid alloy without a stirrer, and recently, Amax Inc. has developed a process involving mixing of particulate reinforcements into molten alloy under conditions of magnetohydrodynamic stirring, followed by direct chill casting of the melt–particle slurry.

Dow Laboratories have used a single-screw extruder (used conventionally for processing polymer products) for synthesizing magnesium alloy-based composites. A schematic diagram of the screw extruder is shown in Fig. 3. Magnesium alloy pellets and reinforcing powders are fed through the feed hopper and the screw acts both as a mixer and a viscosity pump. The slurry of alloy and particles at 580 °C is fed to the die in the exit end of the barrel for casting net-shaped composite products. The process has also been extended to the synthesis of aluminium alloy-based composites. The process variables are rotational speed of the screw and temperature profile inside the barrel.

2.2. Liquid-metal impregnation

2.2.1. Squeeze casting

In squeeze casting [14], a preform or a bed of dispersoids is impregnated by molten alloy under application of hydraulic pressure, as outlined in Fig. 4.

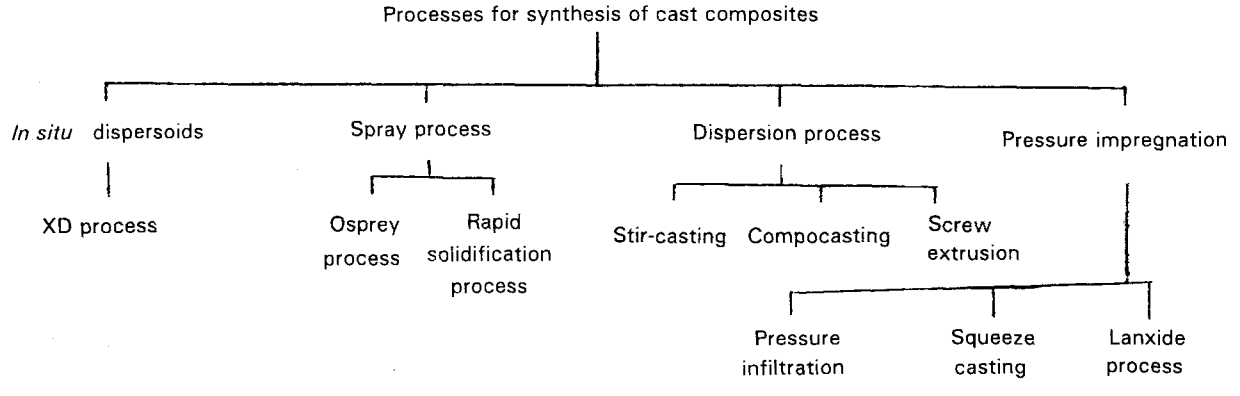

Figure 1 Different casting routes for synthesis of cast metal-matrix composites.

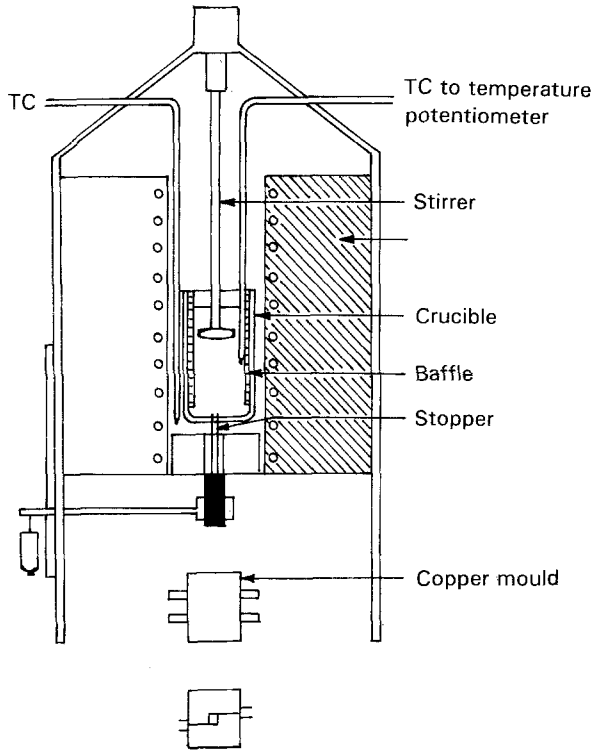

Figure 2 Schematic drawing of apparatus used for stir-casting and compocasting processes. ITC, thermocouple.

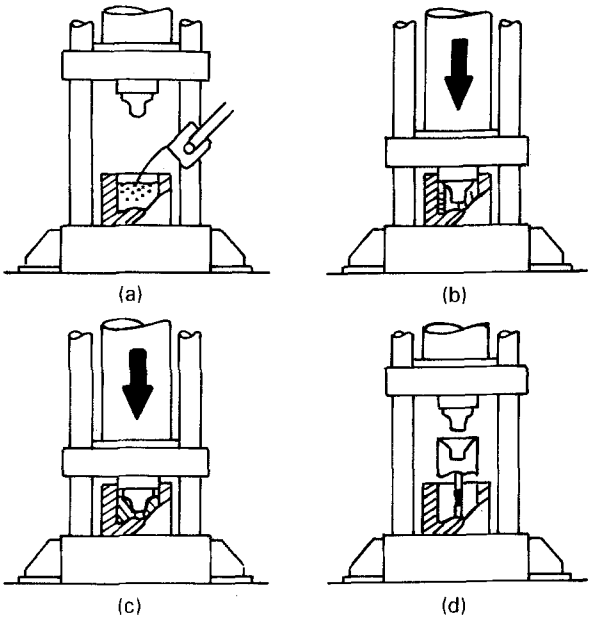

Figure 4 Schematic illustration of different steps in a squeeze-casting process. (a) Pouring, (b) pressurization, (c) solidification, (d) ejection.

The die and preform are initially preheated in order to avoid premature chilling of melt. The plunger is also preheated. The preform fits fairly tightly into the die cavity to reduce the danger of premature melt penetration into the periphery, and the trapping pockets of air within the preform or bed of dispersoids. For each composite system, there is a critical preheating temperature of particles, lower than the liquidus temperature of the penetrating alloy. If the preheating temperature exceeds the liquidus temperature, there will be complete penetration, but molten alloy under high pressure, will leak and splash out of vents and clearances between the plunger and die. The important process variables affecting the quality of squeeze-cast composites are [16]: (a) die preheat temperature, (b) pressure applied, and (c) packing density of the particles in the preform or bed.

2.2.2. Pressure infiltration

In pressure infiltration [15], the hydraulic pressure of squeeze casting is replaced by gas pressure and a schematic drawing of the apparatus is shown in Fig. 5. The main components are a pressure vessel containing the melt in a crucible placed inside a furnace, and a pipe immersed in liquid metal at one end, while the other end is vented to either a neutral atmosphere or a vacuum. A preform or a bed of particles is placed in the pipe blocking the passage. These particles in the pipe are either preheated by immersion in liquid metal or by a separate heater around the segment of the pipe

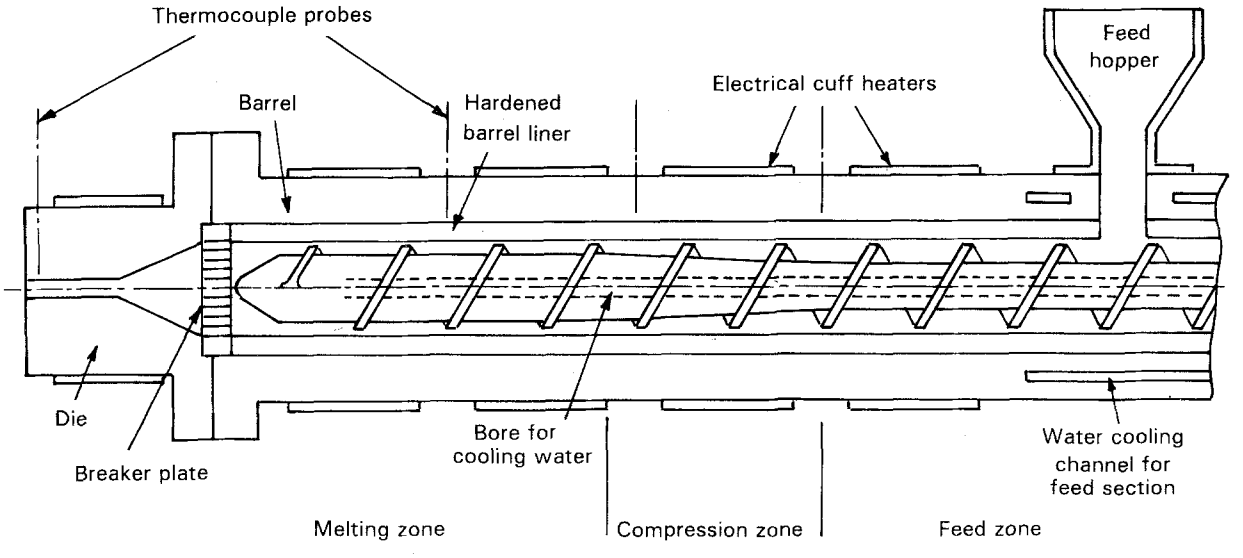

Figure 3 Schematic diagram of a screw extruder.

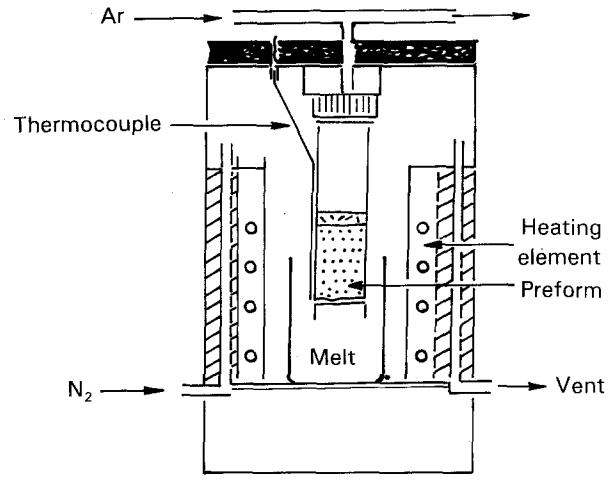

Figure 5 Schematic diagram of a laboratory apparatus for pressure infiltration.

containing the preform or bed. The process variables in pressure infiltration are the same as those in squeeze casting. If the pressure vessel is not pressurized and the end of the pipe is not vented to a neutral atmosphere, but connected to a vacuum line, liquid metal will infiltrate due to the vacuum and the process is called vacuum casting.

2.2.3. The Lanxide process

In the Lanxide process [6], a bed of dispersoid or preform is placed on an alloy ingot and the assembly is heated to a high temperature above the liquidus temperature of the alloy under a controlled atmosphere such as that of nitrogen, as shown schematically in Fig. 6. The alloy should have such a composition that on melting it wets dispersoid particles and infiltrates into the bed or preform without application of pressure. The resulting composite may be made to net or near-net shape by using a suitable preform of dispersoid. The process variables in this process are: (a) infiltration temperature, and (b) particle size, apart from composition of the alloy and the nature of the atmosphere. Here, infiltration takes place almost spontaneously and thus wettability of the dispersoids by the alloy is extremely important.

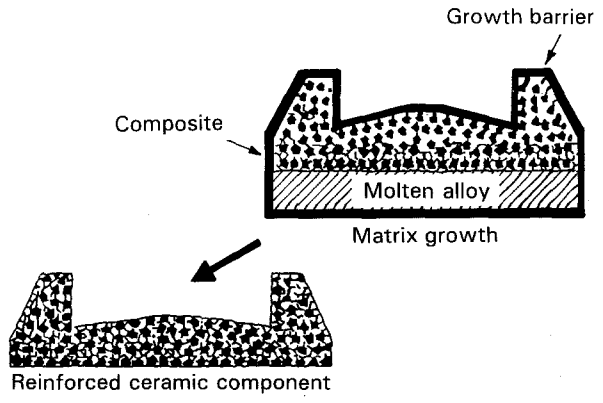

Figure 6 Schematic illustration of the Lanxide process for production of composites.

2.2.4. Principle of molten alloy infiltration

The basic mechanism of all the processes described in Section 2.2, is capillary flow of liquid metals or alloys through channels in the preform or porous bed of particles. Shaler [16] introduced an infiltration index, I, to characterize the tendency of a molten alloy to adhere to a mutual interface with idealized substrate as

$$I = p^2\gamma_{LV}\left[\left(\frac{1}{\phi} - 1\right)(\cos\theta + 1)\right] \quad (1)$$

where ϕ is the volume fraction of porosity in bed, γ_{LV} the liquid–vapour interface tension, θ the contact angle, and p the capillary radius of the channel. A better infiltration is indicated by higher values of infiltration index, I, which results from lowering of the contact angle and porosity.

The kinetics of infiltration in a wetting system has been investigated by several investigators [5, 12, 17]. The net force is equal to the rate of change of momentum during capillary rise. As liquid metal rises in a channel, it is helped by surface tension force and is opposed by force due to gravity, viscous drag and end drag for the configuration given in Fig. 5. If the resultant force is in the direction of capillary rise, infiltration will take place without application of a pressure differential, as happens in the Lanxide process. However, if the resultant force is in the direction opposite to capillary rise, there can be no infiltration without application of a pressure differential required to overcome the resultant opposing force. Thus, there will be a threshold pressure differential below which the resultant force opposing the rise of metal in the channel, will not be overcome, and there will be no infiltration. This picture remains the same even in the case of a non-wetting system with the exception that in the latter case, capillary force will oppose capillary rise of the liquid. The force due to gravity may help or oppose capillary rise depending on the configuration of the preform or bed of dispersoids with respect to the reservoir of liquid metal.

For a small time, t, the infiltration length, h, follows a parabolic law as

$$h^2 = k\,t \quad (2)$$

where k is a positive constant depending on the available effective pressure over and above that required to overcome the resultant force. Below the threshold pressure, k is negative and Equation 2 is not valid. Also, at longer times, Equation 2 is not valid. The rate of capillary rise becomes slower than that predicted by Equation 2 and finally, the equilibrium height, h_e, is reached.

2.3. Spray processes

2.3.1. The Osprey Process

In the Osprey [8, 18] process, a molten metal stream is fragmented by means of a high-speed cold inert-gas jet passing through a spray gun, and dispersoid powders are simultaneously injected as shown in Fig. 7. A stream of molten droplets and dispersoid powders is directed towards a collector substrate where droplets recombine and solidify to form a high-density deposit.

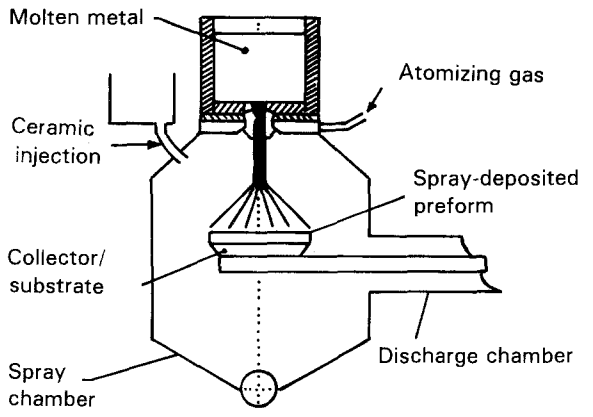

Figure 7 Schematic illustration of the Osprey process.

Dispersoid particles may combine with droplets during flight but most particles are generally co-deposited. Particle spraying can be independently controlled and may be directed to selected areas. The process depends critically on the ability to control enthalpy of droplets in the impinging spray. A droplet should be partially solid when it reaches the substrate. If properly controlled, the process can result in solid deposits in different net shapes of tubes, round billets, strips or clad products. The grain size of the resulting composite is relatively uniform and the presence of particles during solidification of droplets, refines the matrix microstructure. It has also been claimed that there is much less surface reaction or degradation of dispersoid because cold powders are injected. This process is capable of achieving a high rate of production and the deposited product can be directly used in hot-forming such as forging, rolling or extrusion. The process variables are: (a) temperature of the alloy, (b) speed of the gas jet, and (c) temperature of the substrate.

2.3.2. Rapid solidification processing

In rapid solidification processing of composites [19], a jet of liquid alloy–particle slurry impinges under pressure on a water-cooled copper wheel, as shown in Fig. 8, and the resulting flake powders are collected. The flakes are of thickness 40–60 μm, length 6–8 mm and width 0.5–0.7 mm. Two critical processing parameters are speed of the quenching copper wheel and amount of material impinging on this wheel. If the wheel turns too quickly, the slurry will not attach to the wheel long enough to produce a powder. On the other hand, if the wheel is too slow, flakes will be too thick and unacceptable for subsequent processing. The powder is put into cans and consolidated into billet and/or extruded to form a dense composite with higher yield strength, ultimate tensile strength and ductility.

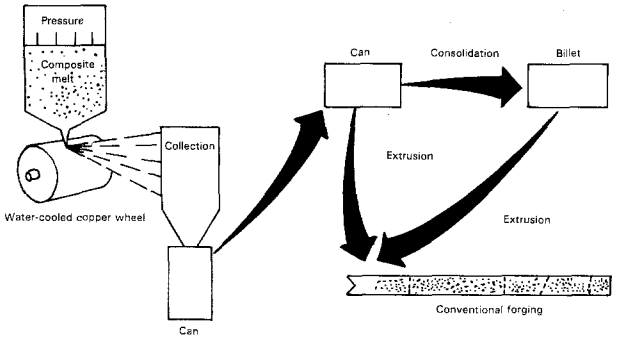

Figure 8 Schematic diagram explaining steps involved in rapid solidification processing of metal-matrix composites.

2.4. In situ production of dispersoids

2.4.1. Chemical reaction in molten alloy

Compound dispersoids such as TiC, TiB_2, TiN and NbB_2, can be produced in an alloy matrix by allowing components to come into contact and react during high-temperature processing in liquid or solid state. The matrix alloy may include aluminium- or copper-based alloys or intermetallic compounds such as aluminides. One of the reacting constituents may remain in solution in the molten matrix alloy and the other constituent may be added as fine powders. A typical example is the formation TiC-reinforced composite by the addition of titanium or ferrotitanium to molten cast iron. It is also possible to use a gaseous reacting constituent, such as acetylene or methane bubbling, in a molten alloy bath containing a carbide former, and chemical reaction may result in fine dispersion of a carbide. The reinforcements can be of various shapes and sizes depending on processing conditions.

Systems for *in situ* production of reinforcements could be designed a *priori* on the basis of thermodynamic and kinetic studies. A reacting constituent, A, may be in solution in a molten alloy, M, and the other constituent may be dispersed as solid particles which may also dissolve in M and react as

$$A(M) + B(M) \rightarrow AB(S) \quad (3)$$

At equilibrium, the free energy change

$$\Delta G^0 = -RTln\left(\frac{1}{a_A a_B}\right) \quad (4)$$

where T is the temperature of the molten alloy, a_A and a_B are activities of A and B in M, and R is the universal gas constant. Whenever activities of A and B are such that

$$a_A a_B > e^{\Delta G^0/RT} \quad (5)$$

there will be formation of compound AB. At higher temperature, the exponential term in Equation 5 will be less, and thus the extent of reaction will be more.

For other types of systems, where there is a reacting gaseous phase or a non-dissolving solid constituent, similar thermodynamic considerations may be worked out to determine the feasibility of *in situ* synthesis of reinforcing compounds. However, the reaction time involved to carry out such synthesis is an important variable to determine cost effectiveness of a process and it cannot be predicted from thermodynamic considerations. Detailed kinetic steps involved in each specific system will have to be examined to determine the overall rate of reaction.

2.4.2. The XD process

In the XD process [7], matrix alloy and reacting constituents are mixed in the solid state and ignited to generate a self-propagating reaction throughout the mixture, as shown schematically in Fig. 9. For the reaction to be self-propagating it has to be exothermic. This process results in stable submicroscopic dispersion of reinforcing particles in a matrix alloy which generally melts at such a high heat as generated by the reaction. Also, high diffusivity of the reacting constituents in the molten alloy helps to bring them together for further reaction and thereby contributes to an increase of the rate of reaction. However, the higher the diffusivities of these constituents, the coarser will

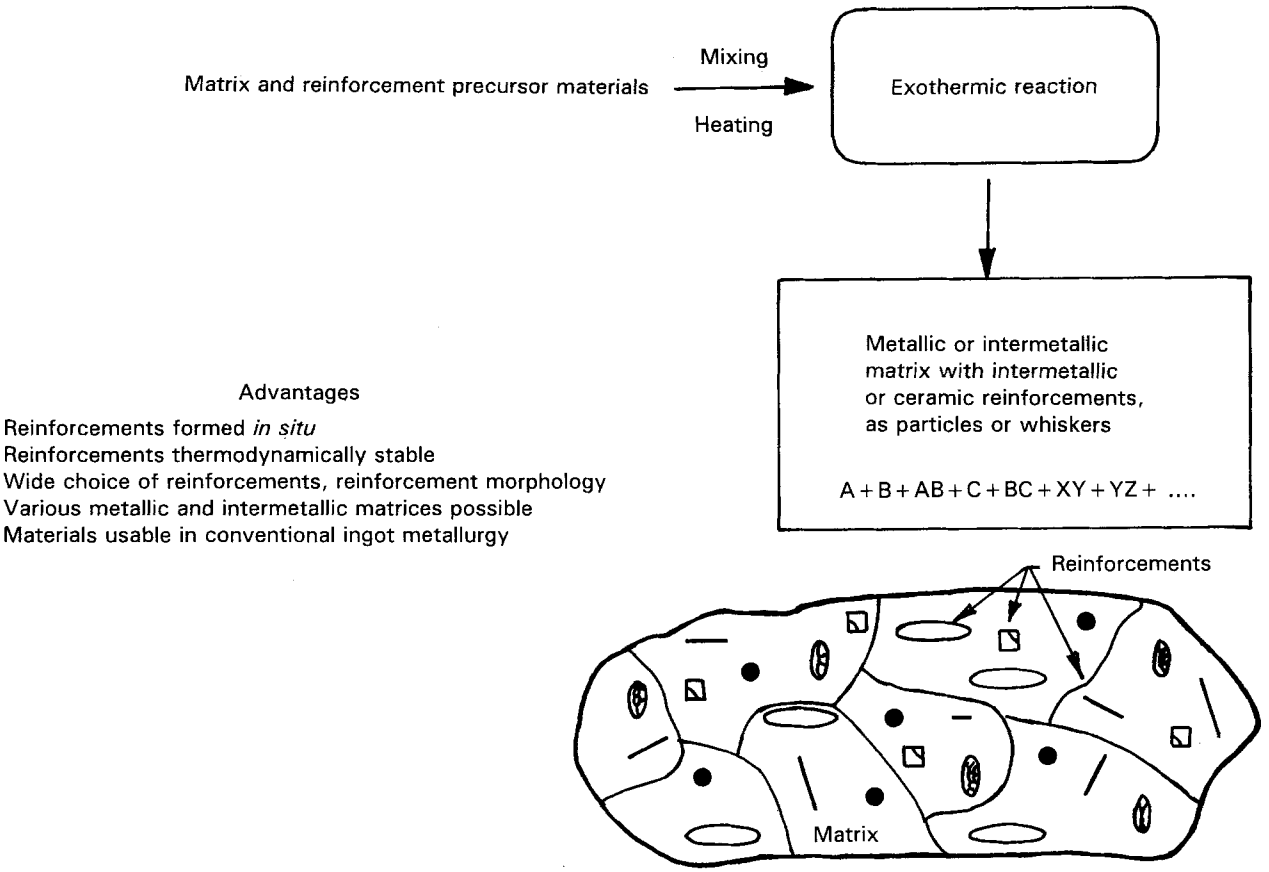

Figure 9 Schematic illustration of the XD process for producing composite materials.

TABLE I Synthesis of cast composites

Period	Location	Composite system	Technique used
1965	Inco., USA	Al/gr	Particle coating and gas injection
1968	IITK, India	Al/Al_2O_3	Magnesium inoculation and stir-casting
1974	IISc, India	Al/SiC; Al/mica	Magnesium inoculation and stir-casting
1975	MIT, USA	Al/Al_2O_3	Magnesium inoculation and compocasting
1978	Hitachi, Japan	Al/gr	Pressure casting
1979	RRL, India	Al/TiO_2; Al/ZrO_2; Al flyash	Magnesium inoculation and stir-casting
1979	USSR	Al/gr	Stir-casting
1983	Martin Marietta, USA	Al/TiC	XD process
1983	Dupont-Toyota	Al/Al_2O_3	Pressure casting
1984	RRL, India	Al/microballoons	Stir-casting
1984	Norsk, Hydro, Norway	Al/SiC	Stir-casting
1985	Iraq	Al/MgO-coated Al_2O_3	Stir-casting
1986	MIT, USA	Al/SiC	Pressure infiltration
1986	DURAL, USA	Al/SiC; Al/Al_2O_3	Stir-casting under reduced pressure
1987	Martin Marietta	TiAl, Ti_3Al/TiB_2 $NiAl/TiB_2$	XD process
1987	MIT, USA	Fe/TiC	*In situ* synthesis
1987	Comalco, Australia	Al/coated Al_2O_3	Stir-casting
1988	Lanxide Corporation USA	Al/Al_2O_3; Al/SiC	Pressureless infiltration
1988	Grenoble, France	Al/SiC	Stir-casting
1988	Drexel Univ., USA	Al/TiC	*In situ* synthesis
1989	Univ. of Wisconsin, Milwaukee, WI	Cu/gr	Stir-casting and compocasting
1989	Honda, Japan	Al/Al_2O_3–C	Pressure casting

be the size of dispersoids; interparticle distance will also increase resulting in lower tensile strength.

The potential of the solidification processing route to the manufacture MMPC lies in its economy over the powder-metallurgy (P/M) method even for small components, such as connecting rods, which can be processed by solidification at roughly half the cost of that involved in the P/M method [20]. This provides justification for development of a host of different methods for the synthesis of cast composites in order to achieve a better product with low cost. Table I lists a variety of different composites developed over the past 25 years. The problems faced during production of these cast composites can be categorized broadly as those causing structural weakness in the product, such as porosity, interfacial reaction, and those associated with its successful casting, such as settling and fluidity. In the following sections, the problems and the measures taken so far to solve them, are described.

3. Structural defects in cast MMPC

When one examines the microstructure of cast MMPC, several structural defects are commonly observed in different systems; porosity, particle segregation and interfacial reactions have drawn considerable attention so far. The present section summarizes the efforts to control these defects.

3.1. Porosity

The mechanical properties of particulate composites are adversely affected by porosity and this damage has several features quite distinct from those of monolithic metals and alloys. At low porosity, one may consider each pore independent of others as inhomogeneous stress distributions around pores are non-overlapping. The damage to mechanical properties, such as ultimate tensile strength (UTS), due to each pore, is additive and UTS is a linear function of the volume per cent of porosity [21]. When porosity increases, there is overlap of inhomogeneous stress distributions around pores and damage becomes a non-linear function of porosity. The influence of shape of the pore may average out and is reflected in the slope of the damage–porosity curve represented by

$$\frac{\sigma_u}{\sigma_0} = 1 - \alpha p \qquad (6)$$

when σ_u and σ_0 are, respectively, the UTS in the presence of p vol % porosity and without it, and α is the characteristic slope, termed the weakening factor. Equation 6 is found to be valid in composites over a much larger range of porosity in composites compared to that in metals and alloys [22]. This has been attributed to screening of the inhomogeneous stress field around a pore by the hard particles embedded in the matrix, thus restricting its spatial range. It explains the dependence of the weakening factor, α, on particle content in a composite, as observed by Ghosh and Ray [22, 23] at both ambient and elevated temperatures, and shown in Fig. 10a and b.

Apart from normal casting porosity resulting from

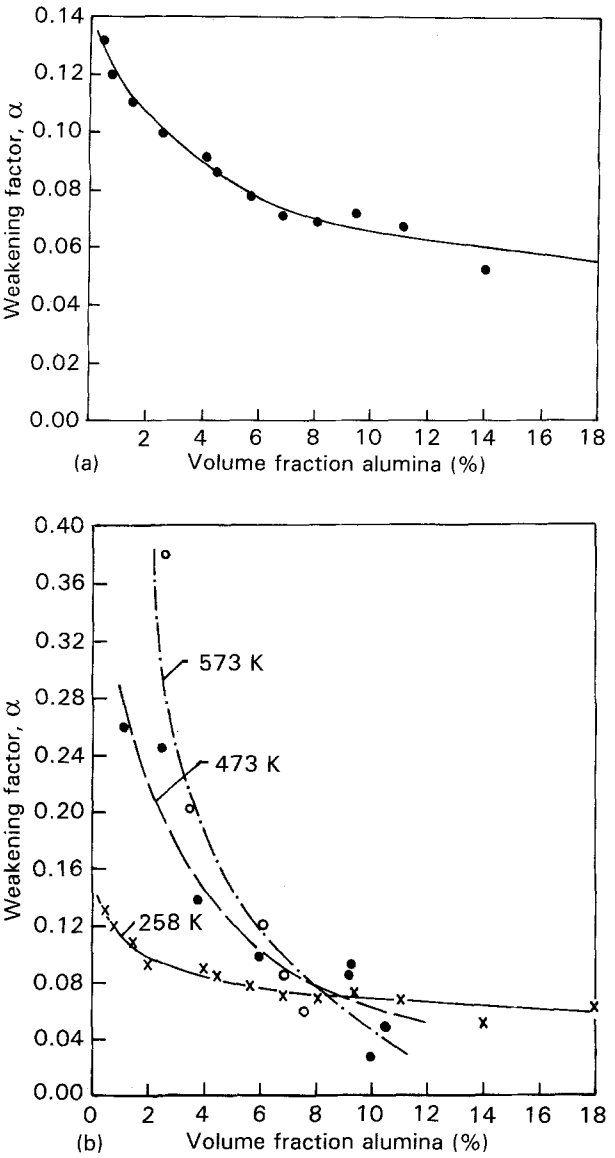

Figure 10 Variation of weakening factor, α, with porosity at (a) ambient temperature, and (b) elevated temperatures.

dissolved gases or shrinkage, there may be additional porosity contributed by the process. In dispersion processes, molten or semi-molten alloy must be agitated to mix dispersoids. The intimate interaction between molten alloy and environmental gases due to agitation, causes enhanced dissolution of gases. Further, if there is a vortex created by agitation, it may cause suction of air bubbles and dispersoids into the molten alloy [24]. The extent of porosity depends on the state of agitation and it can be reduced by control of relevant process variables. Ghosh and Ray [25] have shown the variation of porosity with stirring speed and position of the stirrer as shown in Fig. 11a and b. Thus, one should use a suitable position of the stirrer and stirring speed to reduce porosity. However, it may affect adversely the extent of particle incorporation in the liquid alloy.

In cast composites, porosity can be classified into two types: (a) those away from dispersoids, and (b) those at the boundary of matrix and dispersoids. The latter type of porosity is more undesirable because they aid the debonding of particles from the

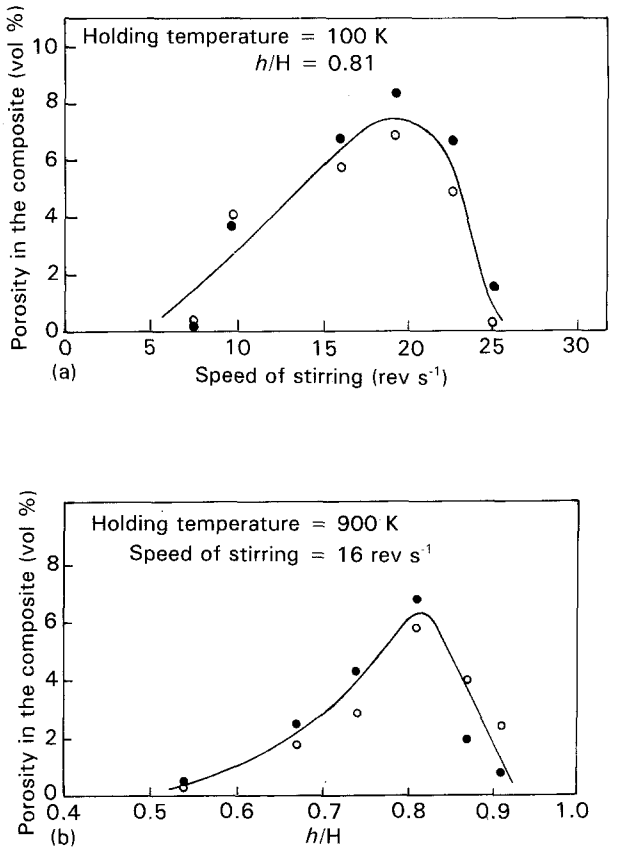

Figure 11 Variation of porosity in $Al–Al_2O_3$ compocast composites with (a) stirring speed, and (b) position of stirrer. (○) Top of casting, (●) bottom of casting, $d/D = 0.63$. d, diameter of stirrer, D, diameter of crucible, h, position of stirrer in liquid from top, H, height of liquid metal in the crucible.

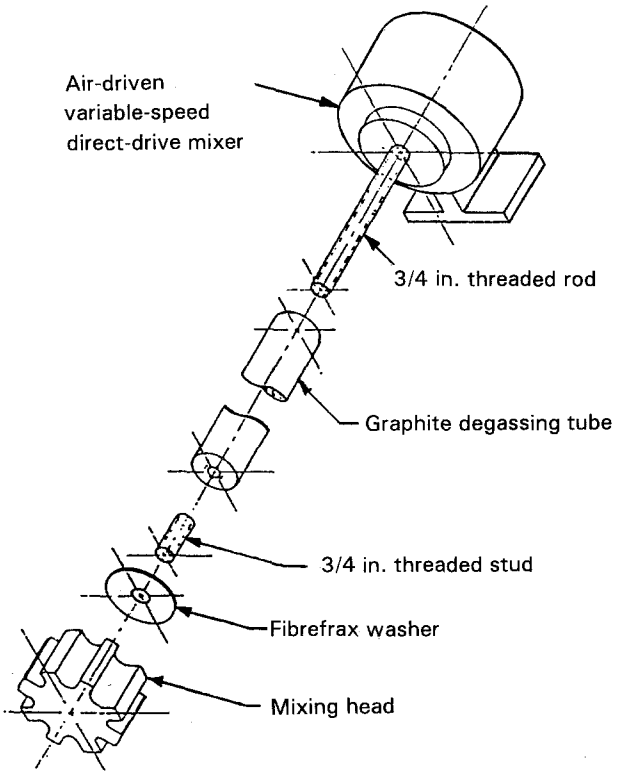

Figure 12 Design of a fluted stirrer for stirring dispersoids in molten alloys.

matrix under low stress. In composites, gas porosity may nucleate heterogeneously on the surface of dispersoids during solidification and help in the flotation of dispersoids. The suction of particles and bubbles together at the vortex, may also result in bubble–particle combinations floating around in the molten alloy. The particles may also become attached to the bubbles, during their movement inside the molten alloy. These mechanisms are primarily responsible for creating porosity at the particle–matrix interface.

In the stir-casting process, there are three possible approaches to reduce porosity: (i) environment control, including application of a vacuum, (ii) use of baffles and improved design of the stirrer, and (iii) maintaining suitable levels of process variables such as stirrer speed, size and position. Duralcan, USA [26], has applied vacuum and inert gas environments while mixing particles with molten alloy in order to reduce porosity in Al–SiC composites. A fluted stirrer [27], as shown in Fig. 12, has been designed again by Duralcan, USA, and it has been claimed that these stirrers leave the top of a melt relatively quiet. Thus, enhanced exposure of fresh liquid alloy to the environment and the resulting increase in dissolution of gases are avoided. Ghosh and Ray [28] have established the existence of maximum porosity corresponding to a definite size, position and speed of the stirrer for a given design of apparatus. However, it has been observed that the same levels of process variables also result in maximum incorporation of particles. Thus, one may not be able to exercise much freedom in changing the process variables to control porosity if, at the same time, the amount of dispersoid incorporation is not sacrificed. Mohan *et al.* [29] introduced ceramic baffles to suppress vortex motion and enhance turbulent mixing.

Caron and Masounave [30] have introduced an interesting variation of dispersion process which has the potential to synthesize low-porosity composites. In this process, particles form a bed at the bottom of the crucible and liquid metal is poured over it. The bed is then sealed by liquid metal for application of vacuum at the bottom as shown in Fig. 13. When vacuum in the bed reaches the desired level, a rotating stirrer is introduced to disperse the bed of particles into the liquid metal. This process is a combination of liquid-metal infiltration to exclude air from the particulate bed, and even dispersion of particles in the liquid metal. Because particles are at the bottom, it will require a high stirring speed to lift up particles for dispersion. Also, the stirring time may be high compared to that required to distribute particles added from the top. The advantage gained by exclusion of air around particles during infiltration in terms of reduced porosity in a composite, may be offset by the requirement of a high stirring speed causing a higher rate of suction of bubbles through the vortex, resulting in an increase in porosity. Thus, in this process, it will be critically important to eliminate the vortex by effective baffling during dispersion of the particles.

In spray casting, the presence of non-interconnected pores has been reported in composites depending on process parameters [31]. The pore-size distribution is reportedly bimodal and different size classes are believed to result from mechanisms such as (a) gas

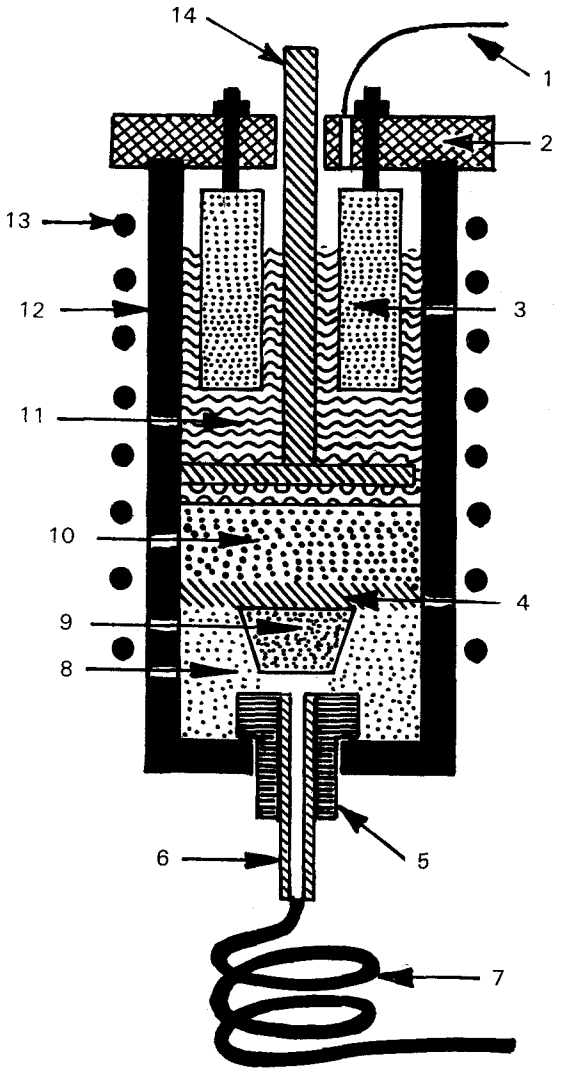

Figure 13 Schematic illustration of a new stir-casting process. 1, Inert gas protection tubing; 2, protection cover; 3, anti-vortex baffles; 4, compressed ceramic fibre disc; 5, ceramic connector; 6, threaded ceramic connector; 7, tubing for inert gas admission and vacuum; 8, structural cement; 9, porous alumina inert; 10, particulate bed; 11, melt; 12, crucible; 13, induction heating coil; 14, stirrer.

entrapment, (b) solidification shrinkage, and (c) discontinuities between spray-deposited particles. All these process parameters which enhance the fraction of liquid in droplets during deposition, result in an increase in porosity. Further investigation into different origins of porosity and measures to be undertaken for its minimization should be carried out to improve the quality of the product.

In melt-impregnation techniques, such as squeeze casting, pressure infiltration or the Lanxide process, the extent of interaction with the environment is much less because there is no agitation like that in dispersion processes. In addition, these processes require isolation and it is possible to control the environment easily. However, these composites are not always free from porosity. There has been very little systematic study on the origin of porosity in these processes, but from stray comments of different investigators, it appears that lack of wetting and the high capillary pressure required to penetrate certain corners in an inhomogeneously packed preform or bed of dispersoids, are the most common causes for porosity in these processes. In addition, if the applied pressure differential is below a critical level, significant amounts of pinhole porosities are observed in cast composites [32].

3.2. Particle segregation

3.2.1. Segregation in slurry

Particle segregation in cast composites could be over either a microscopic scale or a macroscopic scale. The macrosegregation of particles in a composite is generally inherited from inhomogeneous distribution of particles in melt–particle slurries. In stir-casting, the agitator imparts energy to the slurry in the form of eddies and if the scale of eddies is not small enough, it will not be able to break the clusters of particles [29] present. These clusters, if not broken during stirring, will be observed as such in the microstructure of cast ingots as shown in Fig. 14.

El-Kaddah and Chang [33] have dispersed particles in a rotating flow in order to determine the influence of fluid flow on dispersion of particles. Particle lifting in rotating flow is associated with the development of an Ekman boundary layer resulting in secondary flow in the axial direction. For flow in a coaxial rotating cylinder, a particulate dispersion number (PDN) has been defined as the ratio of characteristic velocity in the Ekman boundary layer to the velocity of settling. The PDN is given by

$$\text{PDN} = [H_0(\mu\Omega)^{1/2}]\,[r_i^{1/4} d^{3/4} V_p] \qquad (7)$$

where H_0 is the height of the melt, μ the viscosity of the slurry, Ω the angular velocity of the outer cylinder, r_i the radius of the inner cylinder, d the gap between the inner cylinder and the outer cylinder, and V_p the particle settling velocity. If PDN > 1, the settling velocity is smaller than the axial velocity of the secondary flow and particles will be lifted to the top. On the other hand, if PDN < 1, particles will remain at the bottom. It has been observed that a transition from no particle lifting to particle lifting occurs when PDN is about 4. In the experiments of El-Kaddah and Chang [33], particles which were drilled in a solid

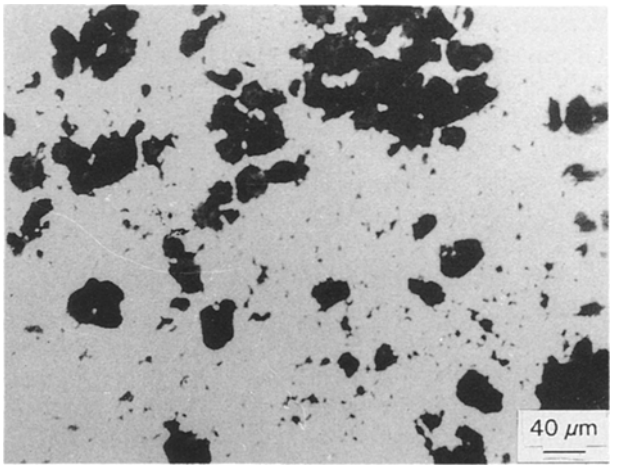

Figure 14 Cluster of alumina particles in a matrix of Al–Mg alloy.

aluminium ingot before melting, could be lifted at a high PDN when the speed of the stirrer was high at 1000–2000 r.p.m. When particles are added from the top, it may be possible to disperse these particles during settling at a much lower stirring speed. In addition, the required stirring time may be reduced and this may be important, particularly when dispersoids react with liquid metal.

3.2.2. Segregation during solidification

Microsegregation of particles may also result during solidification due to pushing of particles by the dendritic solidification front. The earlier studies by Uhlmann *et al.* [34] on the interaction of particles with a planar solidification front, have shown that pushing of particles of given size by the solidification front results when its growth velocity is below a certain critical value. There has not been much further progress in the understanding of this problem because of its complexities involving heat transfer, mass transfer and transient effects. Interfacial energy between particle and solidification front, which cannot be easily measured, is an important factor determining force or energy of interaction between them. In the absence of sufficient theoretical framework, experiments cannot progress beyond a qualitative understanding. The transient effects developing during the contact of a particle with the solidification front, may also be so important in certain circumstances that they determine particle engulfment. There have been three types of approach based on (a) kinetic models, (b) thermodynamic models, and (c) empirical criteria based on heat transfer. All these approaches have succeeded in explaining different aspects of the problem qualitatively, and also sometimes have correctly anticipated the outcome of such particle–front interaction in different systems. However, it is evident that the phenomenon requires an integrated theory involving solidification, heat and mass transfer.

The microstructures of cast particulate composites invariably show that dispersed particles are in the interdendritic region, irrespective of their size [35–37]. It is particularly surprising to observe that large dispersoid particles, which should have a very low critical velocity for engulfment according to our current understanding, are not engulfed by primary phases. Ghosh and Ray [36] have observed that in compocast Al(Mg)–Al_2O_3 composites, particles of intermediate sizes ($\sim$ 4–5 μm) are engulfed by primary α-phase, as shown in Fig. 15, but finer Al_2O_3 particles (< 1 μm) and coarse particles are in interdendritic regions. Thus, it appears that larger particles are surrounded by an interdendritic region not because of particle pushing, but possibly due to its inability to cool down as fast as the liquid alloy away from it. These relatively hotter particles did not allow the liquid in its immediate surroundings, to solidify, and this liquid becomes more enriched in solute because of the progress of solidification elsewhere, as is evident from nucleation of polyhedral silicon in these areas in aluminium A356-based composites.

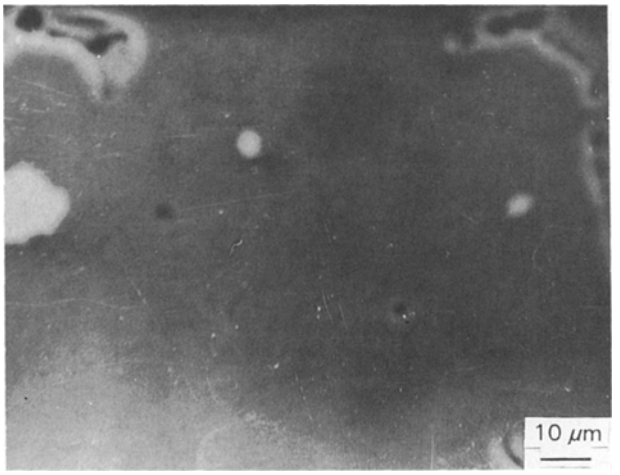

Figure 15 Alumina particle surrounded by primary aluminium phase in compocast Al–Al_2O_3 composite.

During solidification of cast composites, the liquid in front of the dendrites is constitutionally supercooled and the presence of dispersoid particles in this region may promote heterogeneous nucleation. Because no such nucleation of the primary phase has generally been observed, it may be a fair inference that conditions for nucleation on particles are not favourable, due to the relatively higher temperature of the particles. An unfavourable surface-energy balance requiring large undercooling for nucleation, may exclude such a phenomenon in certain systems, but not in general. In the absence of experimental data on solid–solid interface energies between primary phase and a substrate of dispersoids, it is not possible to analyse this situation quantitatively in different systems. However, it has been observed that a number of intermediate phases having high melting points, have nucleated on dispersoids such as silicon on graphite, alumina or SiC particles in Al–Si alloy-based particulate composites, as shown [37] in Fig. 16. Also, an intermetallic phase like Al_3Ni has been found to nucleate on graphite or SiC particles in Al–Nickel-coated graphite or nickel-coated SiC particulate composites.

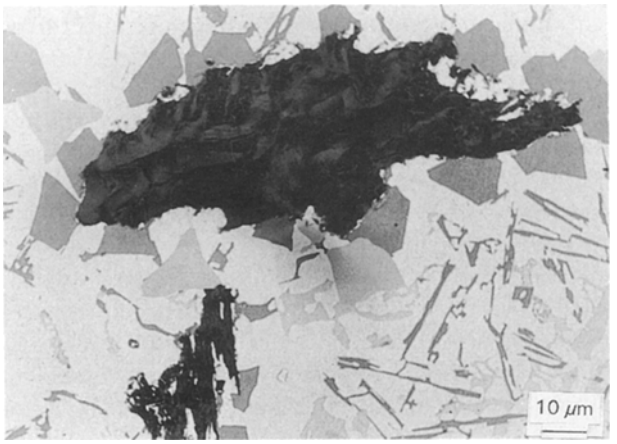

Figure 16 Nucleation of primary silicon around dispersed graphite particles in a matrix of Al–Si alloy.

TABLE II Estimated interface energies in different metal–ceramic systems

System	σ_{DL} (erg cm^{-2})	σ_{DS} (erg cm^{-2})	σ_{SL} (erg cm^{-2})	σ_{DL}/σ_{SL}	σ_{DS}/σ_{SL}
Al–Al_2O_3	1692.8	1366.4	$\geq$ 121	13.99	11.29
Au–Al_2O_3	1660	1710	$\geq$ 132	12.57	12.95
Ag–Al_2O_3	1345	1505	143	9.41	10.52
Cu–Al_2O_3	2067.8	2145	$\geq$ 255	10.36	10.72
Ni–Al_2O_3	2068.1	2475	200	8.10	9.71
Al–SiC	1700	1366.4	$\geq$ 121	14	11.29
Al–Si–SiC	1700	1534.4	$\geq$ 121	14	12.68

Experimental observations of the nucleation of different phases during solidification of dispersoid–molten alloy slurries are quite puzzling. The absence of nucleation of primary phase could also be due to lack of potential for nucleation on the heterogeneous surfaces of the dispersoids. A preliminary analysis could be carried out on the basis of empirical estimates of surface energies for different systems of interest [38]. Some of the surface energies are reported in Table II. σ_{DL}, σ_{DS} and σ_{SL} are dispersoid–liquid, dispersoid–solid and solid–liquid interface energies, respectively, when solid refers to the phase solidifying from the liquid after nucleation on a dispersoid substrate. Both σ_{DL} and σ_{DS} have been normalized with respect to σ_{SL} for various systems, and are plotted in Fig. 17. The centreline with a slope of 1 represents the boundary between $\sigma_{DL} > \sigma_{DS}$ and $\sigma_{DL} < \sigma_{DS}$. The two lines on the two sides of the centreline limit the region where Young's equilibrium equation holds. Region I, adjacent to the vertical axis in Fig. 17, represents a spreading wetting kind of situation between the solidifying phase and dispersoid, where barrierless nucleation will take place. Region II indicates a lack of potency of the dispersoid surface for heterogeneous nucleation. The Young's equilibrium region is marked by heterogeneous nucleation with a reduced barrier height as compared to that in homogeneous nucleation.

The surface energies in Al–Al_2O_3 are such that the primary phase should nucleate all around the dispersed alumina particles. The same conclusion applies for silicon nucleation on a dispersoid of SiC during solidification of Al–Si alloys which has indeed been observed, as shown in Fig. 16. The absence of anticipated nucleation of primary aluminium on dispersoids could be due to questionable empirical estimates of surface energies leading to wrong predictions. However, the same absence of nucleation in a large number of different systems leads one to suspect that there is some other underlying reason. Because ceramic dispersoids used for synthesizing cast composites have lower thermal conductivities compared to those of liquid metals, it is likely that dispersoids will cool relatively slowly compared to liquid metal away from it. The liquid in the immediate surroundings of the dispersoid will also be at a higher temperature. The dendritic solidification, therefore, starts in the liquid away from the dispersoid, and solute rejection accompanying it will enrich the liquid surrounding the dispersoid, resulting in a lowering of its liquidus temperature below its actual temperature. This situation will arise depending on the relative rates of solute rejection and rate of cooling of the liquid around the dispersoids. If the matrix alloy composition is very near the eutectic composition, as in A356 alloy, solute enrichment in the liquid surrounding the dispersoid may take its composition to the hypereutectic side, and the liquidus temperature of this locally hypereutectic alloy will eventually be above the actual temperature of the surrounding liquid. Under such circumstances, separation of primary silicon will take place locally around the dispersoid. If the dispersoid is potent for nucleating primary silicon, as it is for Al–Si alloy-based composites containing SiC, primary silicon will therefore nucleate on dispersoid particles.

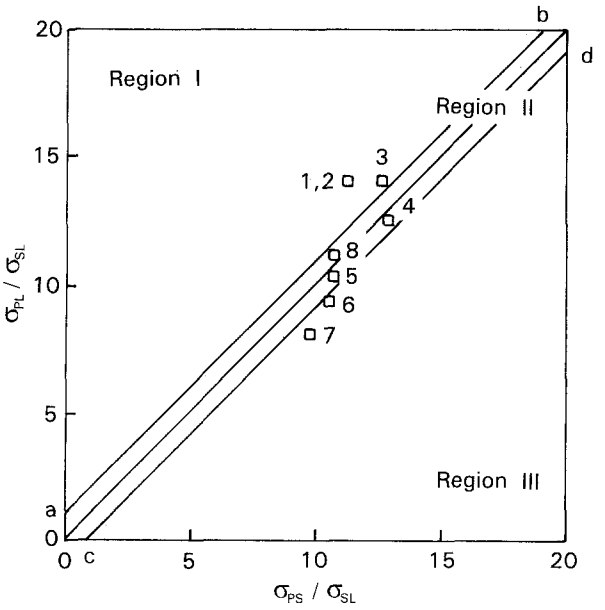

Figure 17 Normalized surface energy plots to determine nucleation behaviour. 1, Al/Al_2O_3; 2, Al/SiC; 3, Al–Si/SiC; 4, Au/Al_2O_3; 5, Ag/Al_2O_3; 6, Cu/Al_2O_3; 7, Ni/Al_2O_3; 8, Fe/Al_2O_3.

Segregation of dispersoids to solute-rich relatively brittle interdendritic regions damages the mechanical properties. The debonding of particles at lower strains, initiates a crack which easily propagates in this brittle region. The progressive debonding of particles leads to a serrated stress–strain curve, as shown in Fig. 18, even before UTS is reached. Particle segregation has been observed both in dispersion and metal impregnation techniques, but in spray casting, it may be possible to avoid segregation.

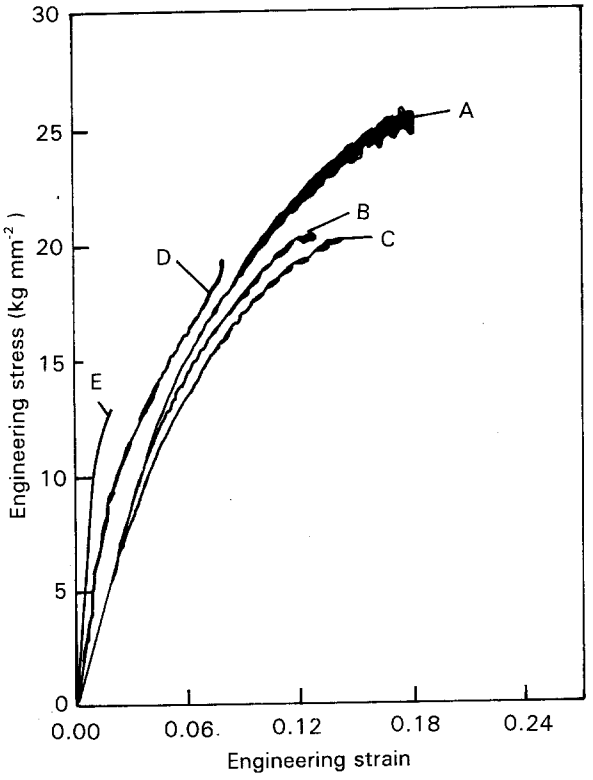

Figure 18 Particle debonding resulting in serrations in the stress–strain curve for Al–Al_2O_3 composite under tension. Volume fraction $Al_2O_3 \simeq 1.92\%$, vol % porosity: (A) 0.06, (B) 0.82, (C) 0.95, (D) 1.5, (E) 6.0.

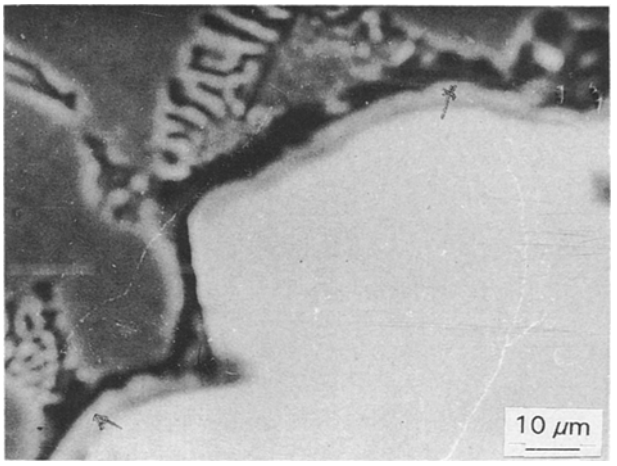

Figure 19 Reaction layer of $MgAl_2O_4$ around an alumina particle dispersed in a matrix of Al–Mg alloy.

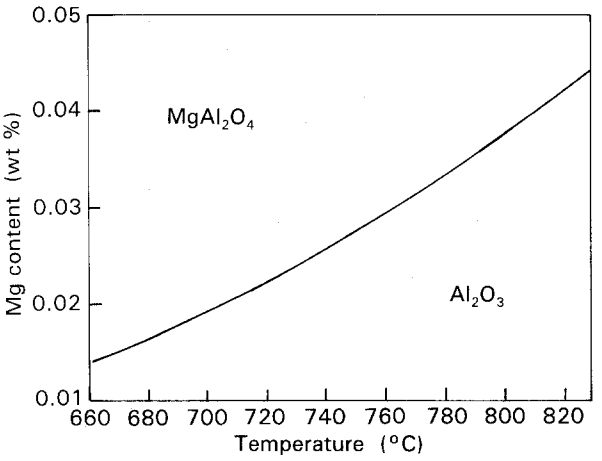

Figure 20 Composition–temperature stability regions for Al_2O_3–$MgAl_2O_4$ equilibria.

3.3. The nature of interfaces and their control

3.3.1. Interfacial reactions

Interfacial reactions may take place either due to the addition of wetting agents or because of direct reaction between dispersoids and base alloy. In 1969, when magnesium was identified by the present author [2] as an element promoting wetting between molten aluminium and alumina, a surface layer of $MgAl_2O_4$, a product of reaction between magnesium and alumina, was immediately observed on the dispersed particles, as shown in Fig. 19. Hikosaka *et al.* [39] have noted the formation of both $MgAl_2O_4$ and $CaAl_2O_4$ on alumina particles when the aluminium alloy contains magnesium as well as calcium. The nature of the reaction depends on the level of magnesium addition in the alloy and the following chemical reactions have been observed

$$3Mg + 4Al_2O_3 \rightarrow 2Al + 3MgAl_2O_4 \quad (8)$$

$$3Mg + Al_2O_3 \rightarrow 2Al + 3MgO \quad (9)$$

The composition/temperature stability for Al_2O_3–$MgAl_2O_4$ equilibria according to Equation 8, has been calculated by McLeod [40] on the basis of free energy of formation of $MgAl_2O_4$ [41] and the published data on activity coefficient [42] of Al–Mg alloys. The results are shown in Fig. 20. Similarly, Al_2O_3–MgO equilibria according to Equation 9, have been analysed to determine the composition–temperature stability regions. The figures indicate that even 0.03 wt % Mg will result in the formation of spinel, $MgAl_2O_4$, during processing of the composite. Thermodynamic calculations indicate that the reaction represented by Equation 8 can proceed in the solid state when the magnesium content of the matrix alloy is lower than that given by Fig. 20 by a factor of 10.

The kinetics of spinel formation has also been investigated by McLeod [40] in Al–1 wt % Mg alloy with 15 vol % alumina stirred at 400 r.p.m., by measuring the magnesium concentration in the matrix alloy after reaction for various times at temperatures between 675 and 800 °C. The extent of reaction is characterized by $\alpha(t)$, as given by

$$\alpha(t) = \frac{W_0 - W(t)}{W_0 - W_e} \quad (10)$$

where W_0 is the initial magnesium concentration in the matrix, W_e the equilibrium magnesium concentration, and $W(t)$ the magnesium concentration in the matrix after reaction for an interval of time, t. Because the surface area of alumina particles is constant and nucleation sites reduce with time, Mampel's model

[43] has been applied

$$\ln(1 - \alpha) = C - 4\pi k^1 N_0 \gamma^2 t$$
$$= k(t_0 - t) \quad (11)$$
$$k = k_0 e^{-Q/RT} \quad (12)$$

where k^1 is the rate constant, C a constant, N_0 the initial surface concentration of nuclei, t_0 the incubation time, k_0 the pre-exponential factor, and Q the activation energy for reaction.

Experimentally it has been found that $k_0 = 50\ s^{-1}$, $Q = 103\ kJ\ mol^{-1}$ and $W_e = 0.03$ approximately, in the temperature range under investigation. Determination of the extent of reaction from the matrix composition may not be very appropriate from the point of view of mechanical properties where the thickness of reacted layer around the particle is relevant. Owing to agitation of the liquid metal during processing, the reaction layer is significantly eroded, and thus the layer thickness cannot be estimated from the change in matrix concentration. Ghosh and Ray [44] have determined the thickness of reaction layer, l (μm), at a temperature, T (K), for a composite synthesized by dispersing 10 vol % alumina in Al–4 wt % Mg alloy by agitation at S r.p.s. as

$$l = 116 - 4.6S \times 10^{-6} \exp(8943/T) \quad (13)$$

A positive $1/T$ exponent in Equation 13 indicates an increased importance of erosion at higher temperature, so that the influence of thermal activation for the reaction has been offset.

There has as yet been no investigation on the extent of magnesium addition required to promote dispersion of alumina in molten aluminium. The rate of reaction will be reduced with lower addition of magnesium, and control of kinetics may pave the way to tailoring quantitatively the mechanical properties of cast Al–Al_2O_3 composites synthesized by magnesium inoculation.

In composites containing silicon carbide particles dispersed in aluminium alloys, there is a surface reaction on the particles, leading to the formation of aluminium carbide [45]

$$4Al + 3SiC \rightarrow Al_4C_3 + 3Si \quad (14)$$

The formation of aluminium carbide degrades reinforcements to affect adversely the mechanical properties, and the composite becomes more susceptible to corrosion. The molten matrix alloy of aluminium dissolves silicon produced by Reaction 14 during synthesis, until the silicon concentration in the alloy reaches the equilibrium value required to suppress further formation of aluminium carbide. Sufficient silicon may be added to the base alloy for it to remain in equilibrium with silicon carbide at the processing temperatures. Fig. 21 shows thermodynamic estimation of the equilibrium silicon content in an alloy required to suppress the formation of Al_4C_3.

The kinetics of Al_4C_3 formation has been investigated by Lloyd *et al.* [46] who observed that its layer thickness, x, on SiC particles cannot be represented by a characteristic parabolic law for diffusion-controlled

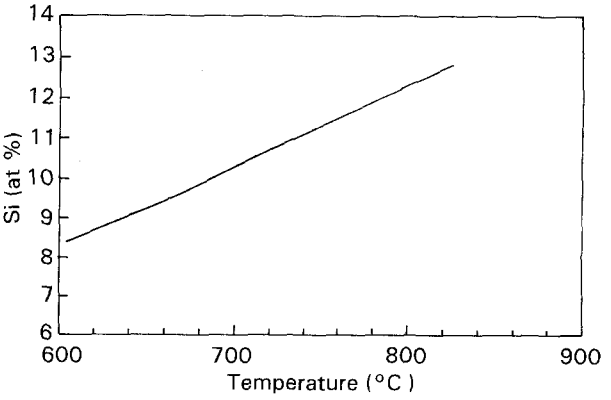

Figure 21 Minimum level of silicon in matrix alloy required to suppress interfacial reaction on SiC in Al–SiC composite.

reaction as given below

$$x^2 = 2k_p t \quad (15)$$

where k_p is a constant and t is the reaction time. It was concluded that nucleation control in the initial stage of reaction is interfering with the parabolic growth law. However, this conclusion may be mistaken, because the growth law is also dependent on the geometry of the particles. Similar diffusion situations have been analysed by Reddi *et al.* [47] for the formation of Nb_3Sn by the bronze route method and where one can explain a non-parabolic growth law for diffusion-controlled reactions. The reaction should be analysed more carefully before drawing any conclusion about the observed non-parabolic growth behaviour of Al_4C_3.

When boron carbide is dispersed in aluminium, the formation of aluminium carbide, aluminium boride and a complex Al–B–C phase occurs at temperatures above 700 °C. It has also been reported that if titanium carbide particles are infiltrated by molten Al–Si alloy, the following reaction takes place [48]

$$13Al + 3TiC \rightarrow 3Al_3Ti + Al_4C_3 \quad (16)$$

Control of the interfacial reactions in a given system can be achieved on the basis of detailed thermodynamic and kinetic considerations. The presence of an interfacial layer of reacted product often impairs the load-carrying capacity of a composite because of debonding of particles at lower loads. Further, a system undergoing such undesirable reactions, should be heat treated only at temperatures where such reactions are extremely slow. Thus, thermodynamic and kinetic studies on these reactions in different composite systems are of considerable technological interest, because, this knowledge will help to control interfacial reactions while processing a cast composite where such reactions are feasible.

3.3.2. Coating of dispersoids and control of atmosphere

The environment during high-temperature processing of a composite may be important because ceramic dispersoids may react chemically or change its stoichimetry. Polymer-derived silicon carbide as in

Tyranno or Nicalon fibres, are unstable at elevated temperatures above 1200 °C, owing to its interaction with the environment during processing or service. The variety of atmospheres tested include nitrogen, argon and carbon monoxide [49]. It was observed that a carbon monoxide atmosphere contributed to an increase in strength of silicon carbide; however, a nitrogen atmosphere resulted in degradation of silicon carbide which may be due to the formation of nitride or oxynitride. However, none of these compounds has so far been detected. The non-reactive atmosphere of argon is next best to carbon monoxide.

In low-silicon or no-silicon alloys, there has been another approach to control interfacial reaction, i.e. by coating. Coating has also been used to promote wetting of dispersoids by a liquid alloy. Electroless copper and nickel coatings have been used widely in the past, but these coatings dissolve easily in aluminium alloys and sometimes there is formation of brittle intermetallic compounds impairing the ductility of the composite. A ceramic coating over silicon carbide has been used to prevent the formation of Al_4C_3. Teng and Boyd [48] used the sol–gel process to coat Al_2O_3 or MgO on silicon carbide which restricts the interfacial reaction. The Naval Research Laboratory (USA) developed single-layer BN and bilayer BN/SiC coatings for polymer-derived SiC [49].

4. Component casting and defects

In all those manufacturing processes where a slurry of liquid alloy and dispersoids is cast by conventional techniques such as casting in sand moulds or permanent moulds, there is often rejection of castings due to highly inhomogeneous particle distribution or defects such as misruns, trapped gases or oxide inclusions. The misruns are due to lack of fluidity of the slurry and the presence of bubbles in the slurry. The problem may arise in different stages of processing, depending on the rheological properties of the slurry.

4.1. Rheological behaviour of melt–particle slurry

A study on the viscosity of slurries in the A356 aluminium alloy–SiC system shows that it is a function of shear rate, temperature and amount of particles in a given system [50]. Viscosities decrease with increasing shear rate as is commonly observed in a shear thinning slurry, and this dependence of non-Newtonian viscosity may be expressed in a power-law form. The viscosity, η, at a given temperature, is given by

$$\eta = A\dot{\gamma}^{(-n)} \tag{17}$$

where A and n are experimentally determined constants. The dependence of viscosity, η, on shear rate, has been attributed to increased orientation of particles and agglomerates in the direction of flow at higher shear rates and also to shearing of agglomerates. The effect of particle content on viscosity is much stronger compared to that of temperature.

Settling or flotation of particles during the remelting of a composite ingot in a furnace or during holding the melt in a ladle for casting, may be a source of inhomogeneous particle distribution in cast components. It is necessary to understand settling or flotation behaviour of a melt–particle suspension in order to control it or to devise a suitable remedial strategy. The Stokes terminal velocity, V_0, of a particle of diameter, d, and density, ρ_p, moving in a melt of density, ρ_m, and viscosity, μ, is given as [51]

$$V_0^2 = \frac{4}{3}\frac{(\rho_p - \rho_m)}{\rho_m}\frac{gd}{C_D} \tag{18}$$

where g is the acceleration due to gravity and C_D is the viscous drag coefficient depending on the particle's Reynolds number, $dV_0\rho_p/\mu$, and a shape factor, ψ, which is the ratio of surface area of a sphere of volume equal to that of the particle and the actual surface area of the particle. For a spherical particle, ψ is obviously 1 and it reduces to 0.847 and 0.806, respectively, for octahedra and cubes. For cylinders, ψ reduce as its height to radius ratio increases, but for discs it is the opposite. There is a significant influence of particle shape on the settling behaviour at a particle's Reynolds number greater than 1. At lower ψ, C_d is higher and the presence of other particles may also reduce settling or flotation velocity of a particle further because of successive collisions during its movement. The velocity of this hindered settling/flotation is given by [52]

$$V_h = V_0(1 - \phi)^n \tag{19}$$

where ϕ is the volume fraction of particles suspended in a melt and n is an exponent observed to be about 4.65. Yarandi *et al.* [53] derived an expression involving the length of the particle-denuded zone in the suspension, h, after a holding time, t, in a melt–particle suspension of depth, H, held in a crucible as

$$t = \frac{H(1 - \phi)^n}{3}V_0\phi(n + 1)\left[1 - \left(1 - \frac{3\phi}{1 - \phi}\frac{h}{H}\right)^{n+1}\right] \tag{20}$$

Another undesirable aspect of particle movement during holding, is cluster formation. The clusters are particles coming together during settling or flotation and are distinct from agglomerates which are permanent. Agglomerates may result from Van der Wall's forces or due to sintering of particles during contact. However, clusters form due to hydrodynamic forces in fluid–multiparticle systems, move together for some time, and disintegrate. Particles aligned vertically often form into clusters because of acceleration of the upper particles due to the wake formed by the lower particles during settling. This wake effect has been observed even at a low Reynolds number of 0.06. At a Reynolds number exceeding 4, the wake effect may draw in particles about ten diameters apart [54].

The rheological behaviour of a melt–particle suspension is also important in the context of casting. The suspension has to flow through a gating system to the mould cavity. During flow, the suspension should

remain homogeneous so that there is no particle segregation inherited in the final cast product. Studies have been conducted on the flow of slurry through pipes [55]. The dynamics of the development of a heterogeneity depend on gravity force acting to settle particles denser than the carrying fluid, and lift forces opposing the action of gravity. Two of the lift forces which are particularly important, are the Bernoulli force caused by a mean velocity gradient across the particle, and the force caused by the spin of the particle giving rise to the Magnus effect. Flow velocity is the most significant variable for maintaining homogeneity of a suspension during flow. The velocity of the molten metal, V, as it enters a runner, may be estimated as [56]

$$V = \frac{[2g(Z - j)]^{1/2}}{n + 1} \tag{21}$$

where Z is the metallostatic head, n a dimensionless number to account for loss of metallostatic head at the entrance ($n = 0.05$ for radial channel and $n = 0.80$ for straight channel), and j the loss of metallostatic head due to surface tension, is given by

$$j = \frac{4\gamma}{a\rho_m g} \tag{22}$$

where γ is the surface tension of the molten metal, ρ_m is its density, a is channel radius and g is acceleration due to gravity. These relations should be appropriately modified for estimating velocity of flow of a melt–particle suspension. Yarandi [57] has measured the velocity of molten A356–SiC suspension in a spiral fluidity channel and found it to be around 40 cm s^{-1}, only 20% lower than that estimated by Equation 22 for base alloy. The studies on flow of suspension in pipes indicate that at a velocity of 30 cm s^{-1}, particles of size 10–100 μm will remain suspended in the carrying fluid. However, in castings, particle segregation is frequently evident [57]. It is possible that particle segregation could have taken place after flow has been blocked due to solidification or during solidification. Also, the conclusions of studies on flow of suspension in pipes, may not be directly applicable in the context of casting, because the channel cross-section here is constantly changing due to solidification and formation of a mushy zone.

Interfacial reaction in alloy–particle slurry is sometimes important in determining casting fluidity [47]. The spiral length of A6061 alloy–15 vol % SiC slurry reduces with increasing temperature up to 740 °C, but beyond this temperature the spiral length reduces. In A6061 alloy there is an interfacial reaction and formation of Al_4C_3, which may cause bridging between particles thus reducing fluidity. However, in silicon-containing A356 alloy, this reaction takes place only above a certain temperature when such a reaction becomes thermodynamically feasible, as explained in an earlier section.

Experimental results on casting fluidity in alloy–particle slurries have been marked by a wide scatter of data on spiral fluidity length [57]. This may be due to particle segregation during flow in channels resulting sometimes in partial hold-up of the flow and resultant build-up of pressure behind it.

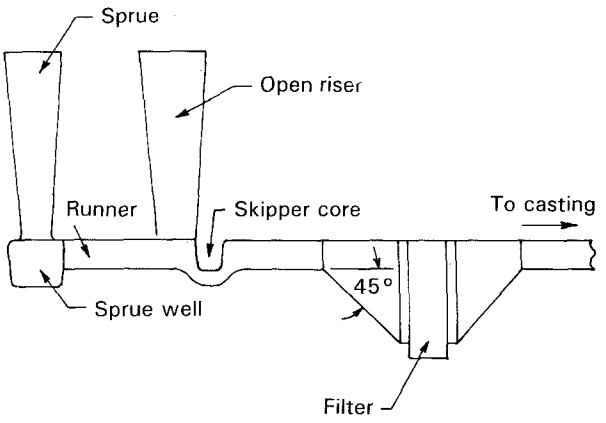

Figure 22 Modification of the gating and risering system recommended for casting alloy–particle slurries.

Surappa and Rohatgi [58] have defined a normalized fluidity which is the ratio of spiral length of the slurry to that of the base alloy. It has been observed that normalized fluidity decreases almost linearly with the specific surface area of the dispersoids in a large number of alloy–particle systems. If these slurries are to be cast by a conventional technique, the particle content must be limited in order to retain the requisite casting fluidity.

The misruns due to trapped bubbles in a slurry can be controlled by appropriate gating and risering [27]. This can be accomplished by placing an open riser and a skimmer core after the sprue well but before the first entry, as shown in Fig. 22. The skimmer core helps to direct bubbles into the riser so that the bubbles can float to surface. The size of the riser is a relevant factor for determining its cleaning ability. The oxide inclusions are removed by using filters if these oxide particles are coarser than the dispersoids.

5. Applications

In spite of three decades of research in the area of cast metal-matrix composites, industrial application of these composites has yet to begin on a regular basis. Several components have been fabricated out of cast composites for various applications, particularly in automobiles, and it has been claimed that these components performed better than those made out of conventional materials (see Table III). Yet, borrowing the phrase of Cornie *et al.* [59], "the future potential of cast composites has not changed its tense to present".

The successful application of cast composites has yet to overcome various technical difficulties described in the earlier sections. There is a lack of investigation on the correlation between process parameters and product quality. It is necessary to carry out these investigations to realize the full potential of a particular technique or its shortcomings.

The application of new materials such as cast composites, will require a host of other developments in related fields. A cast component has to be machined, joined and repaired. Development of suitable tools

TABLE III List of some composite components with proven potential

Composite[a]	Components	Benefits	Manufacturers
Al–SiC(p)	Piston	Reduced weight, high strength and wear resistance	Duralcan, Martin Marietta, Lanxide
	Brake rotor, caliper, liner	High wear resistance and reduced weight	Duralcan, Lanxide
	Prop. shaft	Reduction of weight and high specific stiffness	GKN, Duralcan
Al–SiC(w)	Connecting rod	Reduced reciprocating mass, high specific strength, stiffness and low CTE	Nissan
Mg–SiC(p)	Sprockets, pulleys and covers	Reduced weight high strength and stiffness	Dow Chemical
Al–Al_2O_3(sf)	Piston ring	Wear resistance, high running temperature	Toyato
	Piston crown (combustion bowl)	Reduced reciprocating mass, high creep and fatigue resistance	T&N, JPL, Mahle etc.
Al–Al_2O_3(lf)	Connecting rod	Reduced reciprocating mass, improved strength and stiffness	Dupont Chrysler
Cu–graphite	Electrical contact strips, electronics packaging bearings	Low friction and wear, low CTE	Hitachi Ltd
Al–graphite	Cylinder, liner piston, bearings	Call resistance, reduced friction, wear and weight	Associated Eng., CSIR
Al–TiC(p)	Piston, connecting rod	Reduced weight and wear	Martin Marietta
Al–fibre flax	Piston	Reduced weight and wear	Zollner
Al–Al_2O_3(f)–C(f)	Engine block	Reduced weight, improved strength and wear resistance	Honda

[a] p, particle; w, whiskers; sf, short fibres; lf, long fibres.

and economical methods for machining is mandatory before application, particularly when a composite has hard dispersoids which may damage the conventional tools or reduce its life. The joining of composites may pose problems distinct from those for conventional alloys, because the presence of dispersoids will affect both heat and mass transfer, resulting in a unique microstructure at the joints. A study of these structures and their properties is essential before developing a satisfactory method of joining of a given composite [60].

So far, the main focus of research has been on developing different casting routes for production, and we have, today, a number of different choices, but the relative merits and demerits of different processes, as reflected in product quality or economy, are far from clear. It may be possible to employ some of the as-cast components cast to net shape or near-net shape; but this is an unnecessary limitation on the application of metal-matrix composites. Attention should now be given to heat treatment and bulk deformation processing of cast composites. A superior quality may result after overcoming the limitations of undesirable cast microstructure of composites and casting defects. Investigation on low-speed hot extrusion of cast composites has led to superior mechanical properties and improved fracture toughness [61]. Rolling and forging of cast composites should be carried out to identify desirable conditions and process limitations.

Non-destructive testing of cast composites requires attention for developing suitable methods for quality control [62]. This area generally demands a long experience together with a wide data base. The presence of dispersoids will make it difficult to isolate signals from defects and it may require the devising of some special techniques. The recycling of rejected components calls for a suitable strategy for scrap recycling and some repair technology [63].

At present, it is envisaged that cast composite ingots will be synthesized centrally and supplied to the user industries for remelting of cast ingots to manufacture-cast components. Remelting results in particle settling and clustering. If the quality of a cast component can only be ensured by using all the facilities required to synthesize sound cast ingots, the strategy may have to be revised. The user industry may synthesize the dispersoid–alloy slurry and cast it to final shape on their shop floor. The answer to these various questions [64, 65] will evolve in the near future but the most promising fact of the eighties in the field of cast composites, is the beginning of commercial production of composite ingots. Let us hope that

joining of commercial efforts will take cast composites out of its infancy in the cradles of the research laboratories, to a bright future of widespread industrial application.

References

1. F. A. BADIA and P. K. ROHATGI, *Trans. AFS* **79** (1969) 346.
2. S. RAY, MTech dissertation, Indian Institute of Technology, Kanpur (1969).
3. R. MAHRABIAN, R. G. RIEK and M. C. FLEMINGS, *Metall. Trans.*, **5** (1974) 1899.
4. P. R. PRASAD, S. RAY, J. L. GAINDHAR and M. L. KAPOOR, *Z. Metallk.* **73** (1982) 420.
5. S. RAY, *Ind. J. Technol.* Special Issue on Materials, edited by P. Rama Rao, S. Ray and S. Ranganathan **28** (1990) 368.
6. M. K. AGHAJANIAN, J. T. BURKE, D. R. WHITE and A. S. NAGELBERG, SAMPE Quarterly Vol. 34 (1989) p. 817.
7. L. CHRISTODOULU, P. A. PARRISH and C. R. CROWE, *Proc. Symp. Mater. Res. Soc.* **120** (1988) 29.
8. P. CHESNEY, *Met. Mater.* (1971) 373.
9. E. A. FEEST, *Mater. Design* **7** (1986) 58.
10. T. C. WILLIS *Met. Mater.* **4** (1988) 485.
11. R. MUNRO, in "CIMAC Conference", Oslo, Paper D109 (1985).
12. T. R. FLETCHER, J. A. CORNIE and K. C. RUSSEL, in "Cast Reinforced Metal Composites" edited by S. G. Fishman and A. K. Dhingra (ASM, Metals Park, OH 1988) p. 21.
13. P. K. GHOSH and S. RAY, *Ind. J. Techol.* **26** (1988) 83.
14. A. MORTENSEN, M. N. GUNGOR, J. A. CORNIE and M. C. FLEMINGS, *J. Metals* **38** (1986) 30.
15. J. A. CORNIE, A. MORTENSEN, M. N. GUNGOR and M. C. FLEMINGS, in Proceedings of the Fifth International Conference on Composite Materials", ICCM V, edited by W. C. Harrigan, J. Strife and A. K. Dhingra (1985) p. 809.
16. A. J. SHALER, *Int. J. Powder Metall* **1** (1965) 3.
17. P. B. MAXWELL, G. P. MARTINS, D. L. OLSON and G. R. EDWARDS, *Mater. Trans.* **21B** (1990) 475.
18. E. J. LAVERNIA, *Int. J. Rapid Solid.* **5** (1989) 47.
19. E. L. COURTRIGHT, *Tech. Spotlight, Adv. Mater. Proc.* **11** (1990) 71.
20. Kline and Co. Inc., "Metal Matrix Composites 1989".
21. P. K. GHOSH, P. R. PRASAD and S. RAY, *Z. Metallk.* **75** (1984) 370.
22. P. K. GHOSH and S. RAY, *J. Mater. Sci.* **21** (1986) 1667.
23. *Idem, ibid.* **22** (1987) 4077.
24. S. RAY, in "ASM Proceedings on Cast Reinforced Metal Composites", edited by S. G. Fishman and A. K. Dhingra (ASM, Metals Park, Ohio, 1988) p. 77.
25. P. K. GHOSH and S. RAY, *Trans. Jpn Inst. Met.* **29** (1988) 502.
26. J. A. CORNIE, H. MOON and M. C. FLEMINGS, in "Proceedings of the ASM Conference on Fabrication of Reinforced Metal Composites", Montreal (ASM, Metals Park, Ohio, 1990).
27. R. E. CLARITY, Progress Casting Group, Internal Report 89–142 (1989) p. 8.
28. P. K. GHOSH and S. RAY, *Trans. AFS* **88** (1988) 775.
29. S. MOHAN, V. AGARWALA and S. RAY, *Z. Metallk.* **80** (1989) 612.
30. S. CARON and J. MASOUNAVE, in "ASM Proceedings on Fabrication of Particulates Reinforced Metal Composites", edited by J. Masounave and F. G. Hamel (ASM, Metals Park, Ohio, 1990) p. 107.
31. E. J. LAVERNIA and N. J. GRANT, *Mater. Sci. Eng.* **98** (1988) 381.
32. H. FUKUNAGA, in "ASM Proceedings on Cast Reinforced Metal Composites", edited by S. G. Fishman and A. K. Dhingra (ASM, Metals Park, Ohio, 1988) p. 101.
33. N. El KADDAH and K. E. CHANG, *Mater. Sci. Eng.* **A144** (1991) 221.
34. D. R. UHLMANN, B. CHALMERS and K. A. JACKSON, *J. Appl. Phys.* **35** (1964) 2986.
35. S. RAY, P. K. ROHATGI and P. K. KELKER, Ind. Pat. 1243 505A (1972).
36. P. K. GHOSH and S. RAY, in "Proceedings of the TMS Fall Meeting" Indianapolis, 1989, edited by P. K. Rohatgi (TMS, PA, 1991).
37. P. K. ROHATGI, R. ASTHANA and S. DAS, *Int. Met. Rev.* **31** (1986) 115.
38. L. E. MURR, "Interfacial Phenomen in Metals and Alloys" (Addison-Wesley, MA, 1975).
39. T. HIKOSAKA, K. MIKI and N. KAWAMOTO, *Aichiken Koygo Gijutsu Senta Hokuku* **23** (1987) 41.
40. A. D. McLEOD, in "ASM Proceedings on Fabrication of Particulates Reinforced Metal Composites", edited by J. Masounave and F. G. Hamel (ASM, Metals Park, Ohio, 1990) p. 17.
41. J. L. MURRAY, *Bull. Alloy Phase Diag.* **3** (1982) 60.
42. K. L. MAMPEL, *Z. Phys. Chem.* **A187** (1940) 43.
43. *Idem, ibid.* **A187** (1948) 235.
44. P. K. GHOSH and S. RAY, in "ASM Proceedings on Fabrication of Particulates Reinforced Metal Composites", edited by J. Masounave and F. G. Hamel (ASM, Metals Park, Ohio, 1990) p. 23.
45. D. J. LLOYD, *Compos. Sci. Technol.* **35** (1989) 159.
46. D. J. LLOYD, H. LEGACE, A. McLEAOD and P. L. MORRIS, *Mater. Sci. Eng.* **A107** (1989) 73.
47. B. V. REDDI, S. RAY, V. RAGHAVAN and A. V. NARLIKAR, *Philos. Mag.* **38** (1978) 559.
48. Y. H. TENG and J. D. BOYD, in "ASM Proceedings on Fabrication of Particulates Reinforced Metal Composites", edited by J. Masounave and F. G. Hamel (ASM, Metals Park, Ohio, 1990) p. 125.
49. B. A. BENDER, T. L. JESSEN and D. LEWIS III, *Naval Res. Rev.* **XLII** (1990) 20.
50. F. AJERSCH and M. MADA, Report of CDT Project P1274, Ecole Polytechnique (1989) p. 6.
51. R. C. COX and S. G. MASON, *Am. Rev. Fluid Mech.* **3** (1971) 291.
52. M. E. WOODS and I. M. KRIEGER, *J. Colloid Interface Sci.* **34** (1970) 91.
53. F. M. YARANDI, P. K. ROHATGI and S. RAY, in "2nd International Conference on Processing of Semi-Solid Alloys and Composites", edited by S. B. Brown and M. C. Flemings (MIT Press, MA, 1992) p. 447.
54. Y. CHAN, C. JANG, P. CAI and L. FAN, *Chem. Eng. Sci.* **9** (1991) 2253.
55. G. W. GOVIER and K. AZIZ, "The Flow of Complex Mixtures in Pipes" (Van Nostrand Reinhold, New York, 1992) p. 617.
56. F. R. MOLLARD, M. C. FLEMINGS and E. F. NIYAMA, *Trans. AFS* **88** (1988) 647.
57. F. M. YARANDI, PhD dissertation, University of Wisconsin-Milwaukee (1991) pp. 63, 90.
58. M. K. SURAPPA and P. K. ROHATGI, *Metall. Trans.* **12B** (1981) 327.
59. J. A. CORNIE, A. MORTENSEN, F. FILED and S. STOKES, in "Proceedings of Innovation in Materials and Applications in the Transportation Industries", ATA-MAT (1989).
60. G. F. METZGER, *Weld. Res. Council Bull.* **207** (1975) 171–191.
61. B. N. KESHAVRAN, PhD dissertation, University of Kerala, India (1985).
62. M. EBISAWA, T. HARA, T. HAYASHI and H. USHIO, SAE Technical paper 910835 (1991).
63. S. RAY, *Ind. J. Technol.* **28** (1990) 368.
64. P. K. ROHATGI, R. ASTHANA and S. DAS, *Int. Met. Rev.* **31** (1986) 115.
65. A. MORTENSEN, J. A. CORNIE and M. C. FLEMINGS, *J. Metals* **40** (1988) 12.
66. P. K. ROHATGI, R. ASTNANA, R. N. YADAV and S. RAY, Met Trans. 21A (1989) 2073.
67. M. SUERY and L. LAJOYE, Solidification of Metal Matrix Composites, Ed. P. K. Rohatgi, The Min., Met. and Mat. Soc., (1990) 171.

Received 6 July
and accepted 30 November 1992